Systematic investigation of methods to suppress membrane plasticization during CO_2 permeation at supercritical conditions

Journal of Membrane Science 647 (2022) 120292

Contents lists available at ScienceDirect

Journal of Membrane Science

journal homepage: www.elsevier.com/locate/memsci

Systematic investigation of methods to suppress membrane plasticization during CO_2 permeation at supercritical conditions

Menno Houben, Joey Kloos, Machiel van Essen, Kitty Nijmeijer, Zandrie Borneman *

Membrane Materials and Processes, Department of Chemical Engineering and Chemistry, Eindhoven University of Technology, P.O. Box 513, 5600, MB, Eindhoven, the Netherlands

ARTICLE INFO

Keywords:
CO_2-Plasticization
Supercritical CO_2
Polymer blending
Thermal treatments
Chemical crosslinking

ABSTRACT

The suppression of CO_2-induced plasticization in polyimide membranes at supercritical conditions up to 120 bar is investigated. Three approaches (polymer blending, thermal treatments and chemical crosslinking) known from relatively low-pressure applications are applied and their effectiveness to suppress membrane plasticization at high CO_2 pressures and under supercritical conditions is systematically identified. CO_2 sorption measurements reveal that especially Henry sorption promotes plasticization and that the corresponding Henry sorption parameter (k_D) correlates with the d-spacing and T_g of the membranes. A lower d-spacing and higher T_g results in a reduced k_D parameter and thus a higher resistance to plasticization. A high interchain rigidity is required to suppress plasticization at the highly plasticizing liquid-like CO_2 densities. Chemical and thermo-oxidative crosslinking results in the largest decrease in interchain mobility and therefore shows the highest resistance to plasticization, but also a significantly lower permeability. Thermally treating the membranes in N_2 retains a high permeability, while still displaying significant plasticization resistance. Polymer blending does increase the plasticization resistance, but strongly reduces the permeability. All three methods manage to suppress plasticization at supercritical conditions, but crosslinking offers superior plasticization resistance. However, proper tailoring strategies are required to combine a high plasticization resistance with a high permeability.

1. Introduction

CO_2-induced plasticization presents a great challenge in glassy polymeric membrane gas separations involving high pressure CO_2 [1–5]. High-performance polyimides have excellent separation performance at low pressures for *e.g.* CO_2/CH_4 separations but lose much of their CO_2/CH_4 selectivity at high CO_2 pressures (>30 bar) due to plasticization [6–8]. The polymer matrix swells due to high sorption of CO_2 at high pressure conditions increasing the polymer free volume and chain mobility. As a result, the permeability of all components increases. However, this effect is more dominant for the slower permeating component, thus simultaneously the selectivity decreases. This reduction in selectivity is mainly caused by the loss in diffusion selectivity as the membrane is less able to discriminate effectively based on size and shape due the increased chain mobility. To prevent the loss of membrane selectivity, as relevant for many industrial applications *e.g.* natural gas processing or enhanced methane recovery (CO_2 pressures >80 bar), a higher resistance to plasticization of the membrane is required [6,9–11].

Different approaches can be used to suppress CO_2-induced plasticization, *e.g.* polymer blending [12,13], chemical crosslinking [14,15], thermal treatments [16,17] and UV-crosslinking [18,19]. As extensive detailed literature is available on these approaches, only a short overview of the approaches is presented below.

Through polymer blending, membrane materials can show different properties compared to those of the individual polymers. Therefore, blending polyimides with a high tendency to plasticize with polymers exhibiting a high resistance to plasticization is a relatively easy method to tailor the separation performance of the membrane material. Bos et al. [12] blended polysulfone (PSf) and a polyimide (P84), exhibiting a high plasticization resistance, with the polyimide Matrimid® 5218 (Matrimid), which has a low plasticization resistance. The two homogenous Matrimid/PSf and Matrimid/P84 blends showed a shift of the plasticization pressure to higher CO_2 pressures, indicating an increase in plasticization resistance. However, this increase in plasticization resistance came at the cost of a reduced permeability.

Chemical crosslinking is a practical and widely used method to effectively increase the plasticization resistance and stability of membrane materials [20,21]. Polyimides can be crosslinked by opening of

* Corresponding author.
E-mail address: z.borneman@tue.nl (Z. Borneman).

https://doi.org/10.1016/j.memsci.2022.120292
Received 9 December 2021; Received in revised form 14 January 2022; Accepted 18 January 2022
Available online 21 January 2022

the imide ring using diamine crosslinking agents, where the chemistry and properties of the diamine crosslinker determine the final membrane properties [14,22,23]. Crosslinked polyimide networks exhibit a higher resistance to plasticization due to the strongly reduced chain mobility, but typically have a densified structure and thus reduced permeabilities. A higher degree of crosslinking in general results in a better resistance to plasticization, but also in a larger reduction in permeability [23]. Moreover, polyimide membranes can also be thermally crosslinked at sufficiently high temperatures to suppress plasticization. Bos et al. [6] thermo-oxidatively crosslinked a polyimide at a temperature above the glass transition temperature (T_g) resulting in a reduction of the chain mobility and increase in chain packing, thereby suppressing plasticization.

Besides thermally induced crosslinking, membranes can also be thermally annealed above and below the T_g to improve the plasticization resistance [17,24,25]. These thermal treatments have been utilized to obtain higher packing densities, higher T_g's, lower chain mobilities and thus a higher plasticization resistance. Dong et al. [24] and Zhou et al. [25] studied the thermal annealing of Matrimid hollow fibers at temperatures at both below and above the T_g. Thermal annealing below the T_g resulted in suppression of CO_2-induced plasticization that was strongly correlated with the formation of charge transfer complexes (CTC's). The thermal treatments provide the polymer chains with enough mobility so that the electron-deficient imide ring and the electron-rich aromatic phenylene ring can approach each other allowing the donation of π electrons, forming these CTC's [26]. The formation of these CTC's results in smaller free volumes, reduced polymer chain mobilities and thereby suppressing plasticization. Thermal annealing above the T_g also resulted in thermally induced crosslinking, similar as Bos et al. [6] observed, further increasing the plasticization resistance and selectivity, but simultaneously reducing the permeability. Kita et al. [18] reported the UV-crosslinking of polyimides that contain a benzophenone moiety. Upon UV-irradiation the benzophenone group reacts with hydrogen donating moieties in the polymer chain resulting in crosslinking. Gas permeabilities decreased with increasing UV-irradiation time, while the selectivities increased. However, the plasticization resistance of these UV-crosslinked polyimide membranes is not reported.

Most of the preceding approaches can be effectively used to suppress plasticization at relatively low and moderate pressures (up to 40 bar) but is often paired with a reduction in permeability. Next to that, the extent of plasticization becomes especially more severe at even higher CO_2 feed pressures [5,27]. Previous work clearly shows that such high CO_2 pressures and supercritical conditions extensively impact the plasticization behavior and the separation performance of the polymer membranes [5,28]. CO_2 is in its supercritical state at temperatures and pressures above the critical point (74 bar, 31 °C) where it has considerably different properties than gaseous CO_2 [29]. The CO_2 density was identified as the crucial fluid property influencing the plasticization behavior and thus the CO_2 permeability at supercritical conditions [5,28,30]. In the supercritical region a distinction can be made between a gaseous-like and a liquid-like CO_2 density reminiscent of their subcritical gaseous and liquid domains [31–33]. It is this transition from a gaseous-like to liquid-like CO_2 density that causes a large change in CO_2 density and thus influences plasticization significantly (Fig. 1). The swelling stresses imposed on the polymer membrane at liquid-like CO_2 densities (high CO_2 density) are even higher compared to the swelling stresses at gaseous CO_2 conditions (low CO_2 density) [28]. Obviously, this also impacts methods to suppress plasticization and justifies investigation of the effectiveness of the different methods mentioned above to suppress plasticization at these at highly plasticizing and supercritical conditions.

In this work three established methods are applied to evaluate their plasticization suppression effectiveness at high CO_2 pressures and under supercritical conditions with Matrimid polyimide membranes. Matrimid is very frequently selected as polymer for gas separation membranes. It has excellent performance at lower pressures but a high tendency to plasticize at higher pressures. As a first approach, Matrimid is blended with P84 in various ratios to combine the higher permeability of Matrimid with the plasticization resistance of P84. In a next approach, Matrimid membranes are thermally treated at 350 °C, well above their T_g of 312 °C, in N_2 or air. Finally, Matrimid membranes are chemically crosslinked using two different diamine crosslinkers, m-phenylenediamine and hexamethylenediamine. The resulting membranes are characterized, and the membrane properties are compared to the untreated membranes. All membranes are evaluated for their CO_2 sorption, high-pressure permeation and corresponding plasticization behavior up to 120 bar. The work is concluded with a discussion on the comparison between the three different methods and the crucial material properties required to suppress plasticization at supercritical conditions.

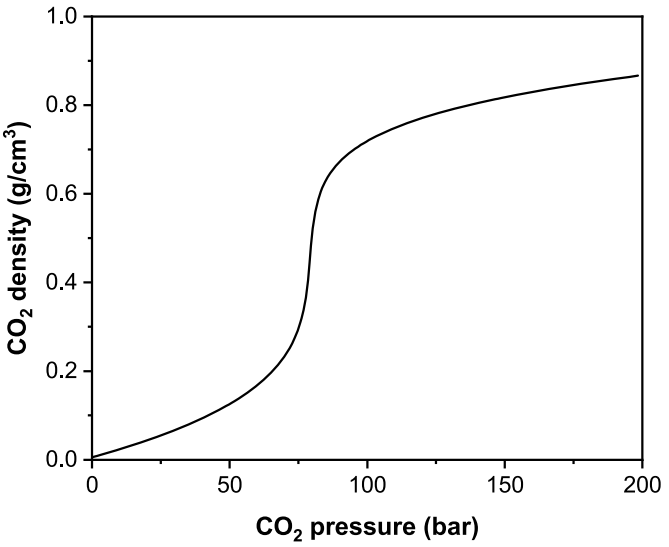

Fig. 1. CO_2 density as a function of pressure at 35 °C. Data are obtained from the database of the National Institute of Standards and Technology [29]. The critical point is at 74 bar and 31 °C. The transition from a gaseous-like to a liquid-like CO_2 density at 35 °C occurs at 80 bar.

2. Experimental

2.1. Materials

The polyimide Matrimid® 5218 (Matrimid) was kindly provided by Huntsman Advance Materials (Switzerland) and P84 was supplied by Evonik GmbH (Austria). Hexamethylenediamine (HMDA, 98%) and m-Phenylenediamine (m-PDA, 99%) diamine crosslinkers were purchased from Sigma-Aldrich. Solvents N,N-dimethylformamide (DMF, ≥ 99.9%), methanol (99.8%) and tetrahydrofuran (THF, 99.8% stabilized with 250 ppm BHT inhibitor) were purchased from Biosolve, The Netherlands. Pure gasses (CO_2 and He) were purchased from Linde Gas (The Netherlands) with a purity of ≥99.995. All chemicals were used as received.

2.2. Membrane preparation

Dense films of the pure polymers were made by casting a 20 wt% solution of the pure polymer in DMF on a glass plate. The films were dried following the same protocol as in our previous work [34]. In short, the solvent was evaporated slowly in a nitrogen atmosphere at room temperature for 48 h. The solidified films were further dried in a nitrogen oven at 80 °C for 24 h, 120 °C for 24 h and 150 °C for 48 h. Casting solutions (20 wt% total polymer in DMF) of the polymer blends were made with various compositions, 25/75, 50/50 and 75/25 g/g Matrimid/P84. Dense films of the polymer blends were dried using the

same protocol as for the pure polymers. The thickness of the resulting films was measured using an IP65 Coolant Proof digital Micrometer from Mitutoyo and was found to be between 40 and 50 μm.

Dried Matrimid membranes were thermally treated in a Nabertherm® muffle oven mounted with a C290 temperature controller at 350 °C in air for 60 min. The heat treatment in air was carried out while the film was still stuck to the glass plate. After the treatment, the films were cooled to room temperature and were released from the glass plate by using hot water. The resulting membrane films were dried in a vacuum oven at 100 °C for 24 h. Additionally, Matrimid membranes were thermally treated in a Carbolite® TZF 12/75/700 tubular oven mounted with a Eurotherm 2132 CP temperature controller under a nitrogen flow of 2 L/min at 350 °C for 60 min. Membranes were sandwiched between two ceramic plates to avoid curling up during the thermal treatment in N_2. After the treatment, the films were cooled to room temperature. The membranes sandwiched between the ceramic plates treated in the tubular oven showed polymer shrinkage and increased in thickness from ~45 μm to ~70 μm.

Pristine Matrimid membranes were chemically crosslinked by immersing the membrane film in a methanol solution containing 10 wt% diamine crosslinker (m-PDA or HMDA) for a stipulated period of time. To remove residual unreacted diamine the membrane films were washed with fresh methanol, followed by drying at room temperature.

2.3. Characterization

Differential scanning calorimetry (DSC) measurements were performed using a DSC Q2000 from TA instruments in the temperature range of 200–380 °C with heating and cooling rates of 5 °C/min. Glass transition temperatures (T_g) were determined using TRIOS software from TA instruments using the 2nd cooling cycle.

Attenuated total reflection fourier transform infrared spectroscopy (ATR FT-IR) spectra were recorded at room temperature on a Varian-cary 3100 FT-IR spectrometer equipped with a golden gate attenuated total reflectance (ATR) sampling accessory. Scans were taken over a range of 4000−650 cm^{-1}, with a spectral resolution of 4 cm^{-1} and 50 scans per spectrum.

Wide-angle X-ray scattering (WAXS) measurements were recorded on a GaneshaLab instrument equipped with a Genix-Cu ultralow divergence source producing X-ray photons of wavelength 1.54 Å and a flux of 108 photons per second. Diffraction patterns were collected on a Pilatus 300 K silicon pixel detector with 487 × 619 pixels of 172 μm^2.

The gel content of the thermally treated and chemically crosslinked membranes was measured by immersion of the membranes in THF for 24 h. The polymer blends were immersed in DMF as pristine P84 has a poor solubility in THF. The insoluble fraction was dried in a vacuum oven at 150 °C for 48 h. The gel content was calculated using the weight of the polymer membrane before and after immersion using Eq. (1).

$$\%gel\ content = \frac{w_1}{w_0} \quad \text{Eq. 1}$$

where w_1 and w_0 are the weight of the insoluble fraction and the original weight of the film respectively.

2.4. High pressure gas sorption

High pressure gas sorption of CO_2 was measured gravimetrically at 35 °C for pressures up to 40 bar for all membranes using a magnetic suspension balance (MSB, Rubotherm series IsoSORP® sorption instrument) equipped with a high pressure syringe pump (Teledyne ISCO 260D). First, the sample was degassed until a constant weight was achieved, followed by a helium pycnometry measurement to determine the initial sample mass and volume. The initial sample mass and volume is used to calculate the density of the sample. Subsequently, the CO_2 sorption is determined at different pressures up to 40 bar by measuring the mass increase in time. The measured mass uptake was corrected for buoyancy according to Archimedes' principle as shown in Eq. (2).

$$m_{CO_2} = m_{meas} + (\rho_{CO_2} \cdot V_s) - m_0 \quad \text{Eq. 2}$$

with m_{CO_2} (g) the buoyancy corrected mass of CO_2 in the sample, m_{meas} (g) the measured mass by the balance, ρ_{CO_2} (g/cm^3) the density of the surrounding CO_2 at the measured pressure and temperature (determined by MSB), V_s (cm^3) the initial sample volume and m_0 (g) the initial mass of the sample. Unfortunately, swelling rates for the modified membranes at high CO_2 pressures are unknown. Therefore, the CO_2 sorption is only measured up to 40 bar as at higher CO_2 pressures the mass uptake needs to be corrected for the swelling dependent buoyancy [5]. The CO_2 concentration in the sample at a specific pressure and temperature was calculated using:

$$C_{CO_2} = \frac{m_{CO_2} \cdot \rho_s}{m_0 \cdot \rho_{CO_2(STP)}} \quad \text{Eq. 3}$$

Where C_{CO_2} (cm^3 (STP)/cm^3 polymer) is the concentration of CO_2 in the sample, ρ_s (g/cm^3) is the density of the sample and $\rho_{CO_2(STP)}$ (g/cm^3) is the density of CO_2 at standard temperature and pressure (STP, 1.013 bar and 273.15 K). The reproducibility of the sorption measurements was assessed by duplicate measurements was found to be within 10% error margin. Because of the very long lead time of the sorption measurements, we decided to carry out more measurements instead of duplicate measurements.

2.5. High pressure gas permeation

High pressure CO_2 permeation was analyzed in a custom-made permeation setup that allows for pure gas measurements on membranes with an effective area of 13.2 cm^2 at pressures up to 120 bar. All measurements were performed at 35 °C. The feed side of the membrane is pressurized using a Teledyne ISCO 500D syringe pump, while the permeate side of the membrane is kept under vacuum. Permeabilities were determined from the steady-state pressure increase in time in a calibrated volume at the permeate side of the membrane. The CO_2 permeabilities were calculated using fugacities instead of pressures, as CO_2 shows strong non-ideal behavior at high CO_2 pressures, as described in our previous work [28]. The equation of state from Soave-Redlich-Kwong was used to calculate the fugacities for CO_2 at 35 °C up to 120 bar [35]. Pressure dependency of the permeability for CO_2 was determined from 20 bar up to 120 bar feed pressure. Permeability values were calculated after 1 h of measurement. For all measurements pristine membranes were taken to exclude any permeation history effects.

3. Results and discussion

3.1. Membrane characterization

First the physical and chemical properties of all membranes are characterized. Results are discussed in the order 1) polymer blending; 2) thermally treated; 3) chemically crosslinked membranes.

3.1.1. Polymer blending

The membrane properties of the polymer blends and the pure polymers are summarized in Table 1. The densities for the pure polymers are comparable to the densities found in literature [12]. The polymer blends have densities in between the densities of the pure polymers (1.23 g/cm^3 for Matrimid and 1.34 g/cm^3 for P84), where increasing the P84 content results in a linearly increasing blend density. Additionally, the Matrimid-P84 blends are optically transparent and have a single T_g indicating a homogenous polymer blend, where the T_g of the blends slightly increases with increasing P84 content (Fig. S1) [36]. However, it must be noted that the difference in T_g between pure Matrimid and P84

Table 1
Density, glass transition temperature (T_g), d-spacing and gel content of the pure polymer and the polymer blend membranes.

Membrane	ρ (g/cm^3)	T_g (°C)	d-spacing (Å)	Gel content (%)
Matrimid	1.23 ± 0.02	312	6.13	0
75–25 M-P84	1.26 ± 0.01	313	6.04	0
50–50 M-P84	1.28 ± 0.01	315	5.87	0
25–75 M-P84	1.30 ± 0.01	316	5.61	0
P84	1.34 ± 0.01	317	5.33	0

is small, also explaining the small change in T_g upon blending (Table 1). WAXS measurements were performed to calculate the average intersegmental spacing or d-spacing in the polymer membranes based on Bragg's law [37,38]. The d-spacing reveals more information on the average available unoccupied volume between the polymer chains [39,40]. Pure Matrimid shows a d-spacing of 6.13 Å, while P84 has a smaller d-spacing (5.33 Å) suggesting a denser polymer packing for P84. In line with expectations, the d-spacing progressively decreases with increasing P84 content, indicating a tighter and narrower structure for the polymer blends compared to pure Matrimid. This reduction in d-spacing is well in agreement with the density data. All polymer blend membranes readily dissolve in DMF, resulting in a gel content of 0%.

3.1.2. Thermally treated

Matrimid membranes have been thermally treated above their T_g at 350 °C for 1 h in an N_2 atmosphere or in an air atmosphere. Fig. 2 presents the ATR-FTIR spectra of pristine Matrimid and the thermally treated Matrimid membranes.

The spectra confirm the preservation of the polyimide structure as the typical imide bonds, 1779 cm^{-1} (Imide C═O symmetric stretch), 1725 cm^{-1} (Imide C═O anti-symmetric stretch), 1374 cm^{-1} (Imide C–N–C axial stretch), 1096 cm^{-1} (Imide C–N–C transverse stretch) and 717 cm^{-1} (Imide C–N–C out-of-plane bending) remain present after the thermal treatment at 350 °C in both N_2 and air [41]. No significant differences between the spectra are observed, suggesting that no significant structural changes occur in the polymer chemistry at these annealing conditions. However, the treated membranes do become partially or completely insoluble in THF after the treatment in N_2 and air respectively, given by the gel content of the membranes in Table 2. This is caused by the formation of charge transfer complexes (CTC's) and/or crosslinking during the thermal treatment [6,17,25,41,42]. Generally,

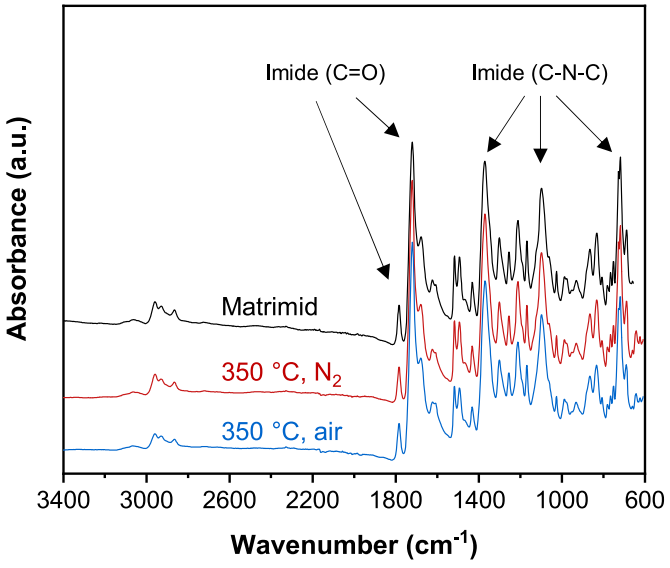

Fig. 2. ATR-FTIR spectra of pristine Matrimid and the thermally treated Matrimid membranes at 350 °C for 1 h in a N_2 or air atmosphere.

Table 2
Density, glass transition temperature (T_g), d-spacing and gel content of pristine and thermally treated Matrimid membranes. Thermal treatments were performed at 350 °C for 1 h in a N_2 or air atmosphere.

Membrane	ρ (g/cm^3)	T_g (°C)	d-spacing (Å)	Gel content (%)
Matrimid	1.23 ± 0.02	312	6.13	0
350 °C, N_2	1.20 ± 0.01	317	6.05	60
350 °C, air	1.18 ± 0.04	319[a]	6.01	>99

[a] The signal of the glass transition is weak.

the formation of CTC's results in an increasing packing density of the polymer chains and restriction of the polymer chain mobility, which suppresses plasticization [25]. Moreover, the yellow color of polyimides is attributed to these CTC's. The color of the pristine Matrimid films is light yellow. The thermally treated films in N_2 have a darker yellow color, while the treatment in air results in a light brown color (Fig. S2). The darker yellow color obtained after the thermal treatment in N_2 suggests a higher concentration of CTC's in the membrane. This is further substantiated by an increase in T_g and a slight decrease in d-spacing for the membranes treated in N_2, which confirms a reduction in chain mobility and a better packing of the polymer chains (Table 2) [6]. These CTC's are known to decrease the solubility of aromatic polyimides [16]. Moreover, it is known that these polyimides can be crosslinked at high temperatures in the solid state [6,24,42]. A mechanism for thermal crosslinking above the T_g in different environments has been given by Kuroda et al. [42]. They suggest that crosslinking occurs by recombination and addition of on-chain radicals, formed by chain cleavage, to the phenyl rings of the polyimide. Above the T_g these crosslinking reactions occur faster due to the high chain mobility, but crosslinking restricts chain mobility again, resulting in relatively low crosslink densities. So, the combination of the formation of CTC's and slight crosslinking resulted in a gel content of 60% for the films treated at 350 °C in N_2.

The gel content for the membranes treated in air (>99%) is significantly higher than the membranes treated in N_2, due to thermo-oxidative crosslinking [42]. In the presence of oxygen higher crosslink densities can be obtained as thermo-oxidative crosslinking proceeds without high mobility of the polymer chains [42]. Further, evidence that the membranes treated in air have a higher crosslink density is that the T_g slightly increases and the d-spacing decreases compared to the membranes treated in N_2. Surprisingly, the density of the thermally treated membranes, both in N_2 and air, decreases with respect to pristine Matrimid. This is not in agreement with the decreasing d-spacing. However, above the T_g the increased chain mobility can result in rejuvenation of the polymer increasing its free volume, thus decreasing its density [41,43,44]. This slight decrease in density and d-spacing upon thermal annealing suggests a redistribution of the excess free volume elements or "microvoids" and the unoccupied space between the polymer chains [24]. This will be further elaborated in section 3.2.

3.1.3. Chemical crosslinking

Matrimid membranes have been chemically crosslinked using two different diamine crosslinkers, a bulky more rigid diamine (m-PDA) and a more flexible diamine (HMDA). ATR-FTIR is used to characterize the degree of crosslinking in the membrane, as the crosslinking reaction leads to the conversion of the imide ring to an amide functionality (Fig. 3). The mechanism of the crosslinking reaction is given in Figs. S3 and S4. As mentioned above Matrimid shows strong imide signals at 1779 cm^{-1} and 1725 cm^{-1} (Imide C═O), 1374 cm^{-1} and 1096 cm^{-1} (Imide C–N–C). Crosslinking Matrimid with m-PDA results in a slight decrease of these imide signals and a slight increase in the signal of the amide peaks at 1667 cm^{-1} (Amide C═O) and 1530 cm^{-1} (Amide C–N) [23,45]. In addition, the signal at 1600 cm^{-1} corresponding to an unreacted amine moiety also increases. Increasing the crosslinking time using m-PDA from 1 day to 7 days results in a minor increase in amide

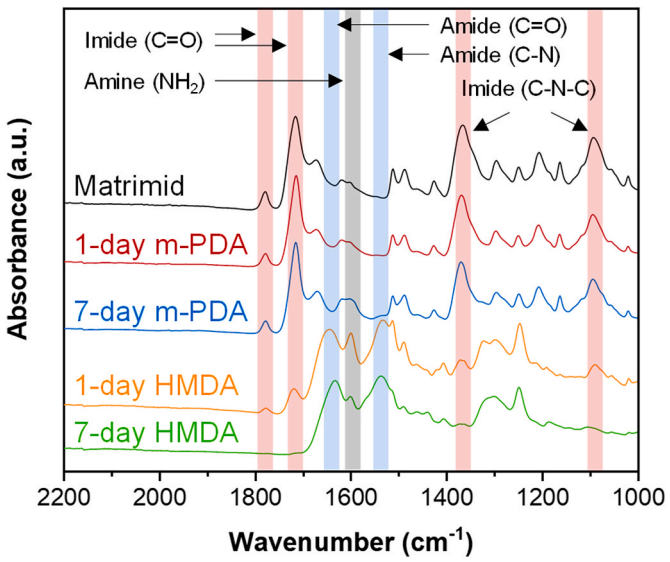

Fig. 3. ATR-FTIR spectra of pristine Matrimid and crosslinked Matrimid membranes using different diamine crosslinkers and crosslinking time.

signals only, indicating a low crosslinking degree. In contrast, crosslinking Matrimid with HMDA gives a much more pronounced change in the ATR-FTIR spectra. Already after 1 day of crosslinking the imide signals almost fully disappear, while strong amide signals appear. However, also a strong signal of the unreacted amine signal (1600 cm^{-1}) remains, which shows that the membrane is not fully crosslinked yet. When the crosslinking time using HMDA is increased to 7 days the imide signals completely disappear, indicating a fully crosslinked membrane.

Images of the crosslinked membranes are presented in Fig. S5. The color of the m-PDA crosslinked membranes changes to light brown and darkens at longer crosslinking times, while the HMDA crosslinked membranes still show a light-yellow color similar to pristine Matrimid. The difference between the two crosslinkers is clearly observed from the resulting membrane properties presented in Table 3. The gel content of the crosslinked membranes using m-PDA is 0%, regardless of the crosslinking time. Although the rate at which the membranes dissolve is slightly delayed compared to pristine Matrimid, the m-PDA crosslinked membranes fully dissolved in THF. This indicates that most of the crosslinking reactions occur at the membrane surface, similarly as observed in literature [23,46]. Even though the membrane is swollen in methanol, it is difficult for the bulky m-PDA to diffuse into the dense Matrimid film, resulting in a low crosslinking degree and thus resulting in a low solvent resistance. The m-PDA crosslinked membranes also show a significant decrease in T_g. The reason for this is the decreasing reactivity of the second aromatic amine group after the first amine of the diamine has reacted with the imide ring [47]. This grafting of m-PDA results in the ring opening of the imide ring providing more chain mobility, but in a low crosslinking degree as it is difficult for two amine groups to react simultaneously on both side of the m-PDA crosslinker.

Table 3
Density, glass transition temperature (T_g), d-spacing and gel content of pristine and chemically crosslinked Matrimid membranes. Matrimid membranes have been crosslinked in a solution of 10 wt% diamine in methanol for a stipulated period.

Membrane	ρ (g/cm^3)	T_g (°C)	d-spacing (Å)	Gel content (%)
Matrimid	1.23 ± 0.02	312	6.13	0
1-day m-PDA	1.17 ± 0.03	296	6.01	0
7-day m-PDA	1.17 ± 0.02	294	6.01	0
1-day HMDA	1.18 ± 0.01	314[a]	6.09	85
7-day HMDA	1.09 ± 0.03	321[a]	5.26	>99

[a] The signal of the glass transition is weak.

On the other hand, HMDA crosslinked membranes show a gel content of 85% after 1 day and >99% after 7 days. This shows that HMDA diffuses easier into the interior of the Matrimid membrane resulting in a higher crosslinking degree throughout the membrane. Further proof for a higher crosslinking degree of the HMDA crosslinked membranes is given by the increased T_g and the reduced d-spacing, especially after 7 days of crosslinking. All crosslinked membranes show a lower density compared to pristine Matrimid, where a higher crosslinking degree results in a lower density. This is attributed to the swelling of membrane film by methanol during the crosslinking reaction [46].

From the comparison of the membrane properties of the treated membranes as discussed above, it is evident that all methods attempt to increase the inter- and intrachain rigidity and to increase the packing density of the polymer chains. Most of the treated membranes show an increase in T_g and/or a decrease in d-spacing. This elucidates that the mobility of the polymer chains is dramatically restricted. It is expected that the rigid conformation provides an enhanced resistance to the high swelling stresses imposed by high CO_2 pressures and supercritical conditions, with the crosslinked membranes showing the highest resistance to plasticization thanks to the high rigidity of a highly crosslinked polymer network.

3.2. CO_2 sorption

Plasticization phenomena scale with the CO_2 concentration in the membrane and thus are closely related to the CO_2 sorption in the membrane [5,27,28]. The experimentally determined CO_2 sorption for all different membranes is presented in Fig. 4a (polymer blending), b (thermally treated) and c (chemically crosslinked). All membranes show the non-linear sorption behavior typically observed for glassy polymers and that can be well described with the dual mode sorption model [48–50]. Fitting the sorption data with the dual mode sorption model provides the dual mode sorption parameters summarized in Table 4 (polymer blending), 5 (thermally treated) and 6 (chemically crosslinked).

3.2.1. Polymer blending

Matrimid shows a higher CO_2 sorption than P84. So as expected, the sorption of the blend membranes is in between the sorption of the two pure polymers, where the CO_2 sorption decreases with increasing P84 content. Especially the Henry's law constant (k_D), which correlates to the CO_2 dissolved in the polymer matrix, decreases with higher amounts of P84 in the polymer blend (Table 4). This reduction in k_D results in a lower slope of the CO_2 sorption (in the linear region) as a function of pressure with increasing P84 content. The Langmuir sorption parameter C'_H and b relate to the sorption in the "microvoids" or unrelaxed free volume of the glassy polymer [49]. This C'_H parameter shows only minor changes for the polymer blends, as the amount of excess free volume is similar for Matrimid and P84. The density and d-spacing data correspond well with the decreasing k_D parameter (Table 1). The denser chain packing for the blends with increasing P84 content, indicated by the lower d-spacing, results in a lower sorption between the polymer chains, thus decreasing the k_D parameter. The Langmuir affinity constant b, which represents the tendency of CO_2 to sorb in the microvoids, is lower for the polymer blends, but shows no significant trend [51]. As P84 shows the lowest increase in CO_2 sorption with pressure (lowest k_D parameter), it is expected that increasing the P84 content in the blend membrane results in a higher resistance to plasticization.

3.2.2. Thermally treated

The thermally treated Matrimid membranes show a decreased CO_2 sorption over the entire pressure range compared to pristine Matrimid (Fig. 4b). Furthermore, the thermal treatment in air results in a larger decrease of CO_2 sorption compared to the thermal treatment in N_2. The reduction in CO_2 sorption is attributed to the formation of CTC's and slight crosslinking, which primarily reduces chain mobility and slightly

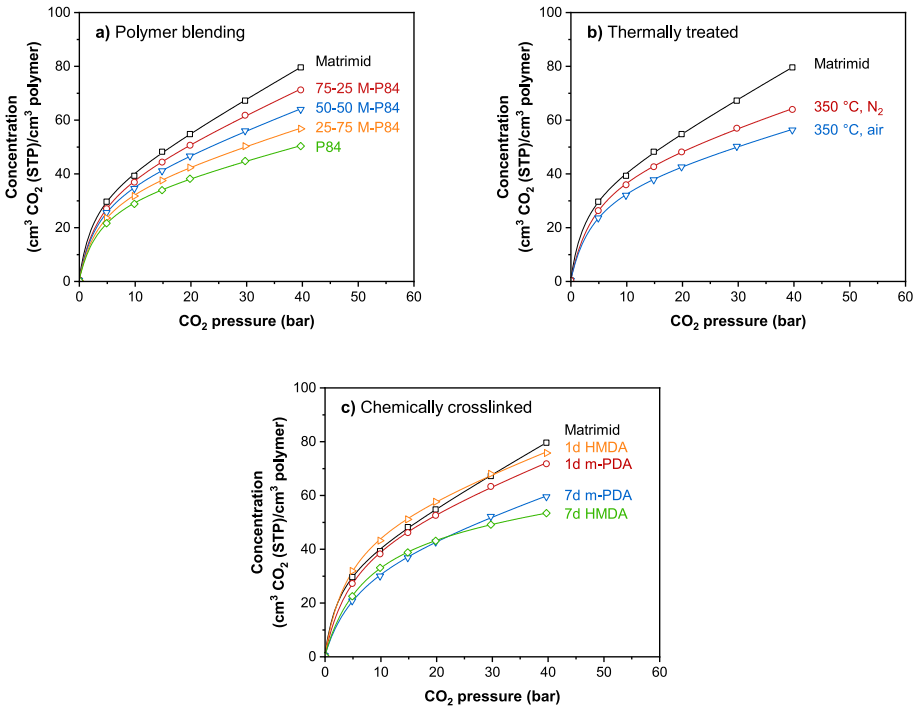

Fig. 4. CO_2 sorption isotherms at 35 °C for **a)** the polymer blend membranes, **b)** the thermally treated Matrimid membranes and **c)** the chemically crosslinked Matrimid membranes. Solid lines are obtained by fitting the dual-mode sorption model. The open symbols represent the gaseous CO_2 phase.

Table 4
Dual mode sorption parameters of CO_2 for the pure polymers and the polymer blend membranes.

Membrane	C'_H [cm^3(STP)/cm^3]	b [1/bar]	k_D [cm^3(STP)/cm^3•bar]
Matrimid	35.18 ± 1.58	0.40 ± 0.06	1.16 ± 0.03
75–25 M-P84	37.37 ± 1.46	0.29 ± 0.03	0.92 ± 0.03
50–50 M-P84	36.38 ± 1.25	0.29 ± 0.02	0.76 ± 0.02
25–75 M-P84	35.22 ± 1.29	0.27 ± 0.03	0.62 ± 0.03
P84	32.65 ± 1.18	0.27 ± 0.03	0.51 ± 0.03

reduces the d-spacing [6]. The reduced chain mobility tends to decrease the dissolution of CO_2 between the polymer chains, which is clearly observed by a decreased k_D parameter in Table 5 [21]. The higher crosslink density obtained during the thermal treatment in air results in a further reduction in the polymer chain mobility and thus decreases the k_D parameter further. Even though the d-spacing of the thermally treated membranes slightly decreases, suggesting a better chain packing, the density decreases as well (Table 2). Similarly, the Langmuir sorption parameter C'_H increases for the thermally treated membranes. This indicates a redistribution of the free volume elements [21,24]. The smaller d-spacing and k_D parameter show that the average unoccupied space between the polymer chains decreases, while the increase in the C'_H parameter shows that the excess free volume (microvoids) becomes larger, resulting a slight decrease in density. It is known that sorption in the excess free volume (Langmuir sorption sites) does not contribute to plasticization [21,52,53]. Therefore, this redistribution between the Langmuir and Henry sorption sites could be beneficial for the plasticization resistance of the membranes. Similar to the polymer blends, a reduction in the b parameter is observed for the thermally treated membranes. It is hypothesized that the thermally treated membranes with a lower k_D value show a higher resistance to plasticization and the diffusion selectivity is preserved at higher CO_2 pressures. At the same time, a higher C'_H value keeps the solubility relatively high, retaining a high permeability.

Table 5
Dual mode sorption parameters of CO_2 for pristine and thermally treated Matrimid membranes. Thermal treatments were performed at 350 °C for 1 h in a N_2 or air atmosphere.

Membrane	C'_H [cm^3(STP)/cm^3]	b [1/bar]	k_D [cm^3(STP)/cm^3•bar]
Matrimid	35.18 ± 1.58	0.40 ± 0.06	1.16 ± 0.03
350 °C, N_2	42.55 ± 1.70	0.23 ± 0.02	0.64 ± 0.04
350 °C, air	37.44 ± 1.37	0.24 ± 0.02	0.56 ± 0.03

3.2.3. *Chemically crosslinked*

Fig. 4c shows the CO_2 sorption of the chemically crosslinked Matrimid membranes. Crosslinking Matrimid with m-PDA results in a reduced CO_2 sorption compared to pristine Matrimid, where increasing the crosslinking time from 1 to 7 days leads to a larger decrease in sorption. Even though the chain mobility of the m-PDA crosslinked membranes is higher compared to pristine Matrimid, indicated by the decreasing T_g (Table 3), the average d-spacing slightly decreases due to crosslinking at the membrane surface. As a result, the dissolution of CO_2 between the polymer chains (k_D) is lower (Table 6). On the other hand, inserting the bulky m-PDA group in the polymer increases the excess free volume resulting in a larger C'_H parameter. Increasing the crosslinking time for m-PDA from 1 day to 7 days leads to a further reduction in both k_D and C'_H parameter, which is attributed to a higher amount of grafted m-PDA and slightly higher crosslinking density at the surface of the membranes. The lower chain mobility of the m-PDA crosslinked membranes also

Table 6
Dual mode sorption parameters of CO_2 for pristine and chemically crosslinked Matrimid membranes. Matrimid membranes have been crosslinked in a solution of 10 wt% diamine in methanol for a stipulated period.

Membrane	C'_H [cm^3(STP)/cm^3]	b [1/bar]	k_D [cm^3(STP)/cm^3•bar]
Matrimid	35.18 ± 1.58	0.40 ± 0.06	1.16 ± 0.03
1-day m-PDA	45.95 ± 2.16	0.20 ± 0.02	0.78 ± 0.04
7-day m-PDA	37.38 ± 2.52	0.17 ± 0.02	0.68 ± 0.05
1-day HMDA	51.54 ± 2.56	0.24 ± 0.03	0.74 ± 0.05
7-day HMDA	53.16 ± 1.34	0.14 ± 0.01	0.21 ± 0.02

causes a reduction in the b parameter. The CO_2 sorption of the HMDA crosslinked membranes show a different trend. The 1-day HMDA crosslinked Matrimid films show a higher initial CO_2 sorption, but a substantially lower increase with pressure compared to Matrimid. These membranes also have a significantly larger C'_H parameter due to swelling of the membrane during the crosslinking reaction (Table 6). This results in a larger initial CO_2 sorption as at low pressures sorption predominantly takes place in the Langmuir sorption sites [46,50,54]. Furthermore, even though the membranes have a higher crosslinking density (gel content ~85%) compared to the m-PDA crosslinked membranes, the d-spacing of the 1-day HMDA crosslinked membranes only decreases marginally compared to pristine Matrimid and is higher than the d-spacing of the m-PDA crosslinked membranes (Table 3). As a result, the 1-day HMDA crosslinked membranes exhibit a k_D parameter similar to the m-PDA crosslinked membranes, while the b parameter increases slightly. The higher crosslink density (gel content >99%) obtained for the 7-day HMDA crosslinked membranes predominantly reduces the chain mobility and d-spacing, which is also expressed by a large decrease in k_D parameter and thus a greatly reduced CO_2 sorption.

It very is clear that all different methods reduce the CO_2 sorption at higher pressures, which is expressed by a decrease in the k_D parameter. This parameter is affected by the average d-spacing of the membrane, where a smaller d-spacing results in a lower k_D parameter. The polymer blends show a clear correlation between the d-spacing and the k_D parameter, as shown in Fig. S6. However, no clear correlation could be found when taking all treated membranes into account. Membranes with similar d-spacings (P84 and the 7-day HMDA crosslinked Matrimid) have significantly different k_D parameters, 0.51 and 0.21 respectively. The reason for this difference is that the membranes have different T_g's (317 °C for P84 and 321 °C for 7-day HMDA crosslinked Matrimid) and thus a different chain mobility. This indicates that the dissolution of CO_2 between the polymer chains is not only determined by the d-spacing, but also affected by the chain mobility (T_g) of the membranes. Considering that plasticization is mostly caused by the dissolution of the CO_2 between the polymer chains, the CO_2 sorption measurements elucidate that the combination of d-spacing and chain mobility are key parameters to reduce the extent of plasticization [21,52,53]. Therefore, it is expected that the highly crosslinked membranes, 350 °C air treated Matrimid and the 7-day HMDA crosslinked Matrimid membranes, have a high resistance to plasticization as these membranes show a low k_D parameter combined with a strongly reduced chain mobility. Previous work shows that the CO_2 sorption in Matrimid membranes at liquid-like CO_2 densities reaches a plateau value and cannot be described with the dual-mode sorption model anymore [5,28]. It is hypothesized that this is also the case for the treated membranes in this work, but that the plateau value is different for all treated membranes. Unfortunately, it was not possible to measure the CO_2 sorption at pressures above 40 bar, as the swelling rates required to correct for swelling dependent buoyancy at these high pressures are unknown for the treated membranes [5]. However, the dual-mode sorption parameters measured in the gaseous CO_2 region combined with the high-pressure permeation behavior still provide useful information on the extent of plasticization at liquid-like CO_2 densities.

3.3. High pressure CO_2 permeation at supercritical conditions

Fig. 5 shows the absolute CO_2 permeability as a function of pressure for all different membranes. The CO_2 permeability was measured in both gaseous CO_2 densities (open symbols, 20–60 bar) and in liquid-like CO_2 densities (closed symbols, 80–120 bar). All permeability measurements are carried out at 35 °C, which means that the transition from a gaseous CO_2 density to a liquid-like CO_2 density occurs at 80 bar.

All CO_2 permeabilities are measured above the plasticization pressure of pristine Matrimid (10 bar), hence the effects of plasticization should be clearly visible [1]. At gaseous CO_2 densities, the CO_2 permeability of Matrimid progressively increases with increasing feed pressure because of plasticization. As previously stated, the extent of plasticization is correlated with the CO_2 concentration in the membrane [5,27]. Accordingly, at higher CO_2 feed pressures the CO_2 concentration in the Matrimid membrane increases resulting in a more plasticized membrane

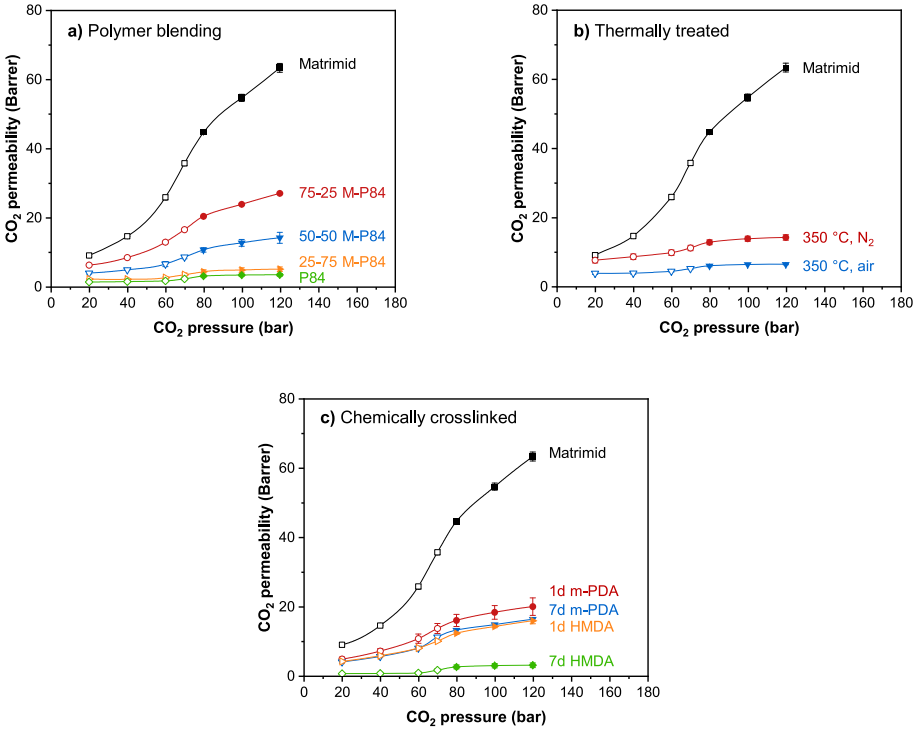

Fig. 5. CO_2 permeability (based on CO_2 fugacity) at 35 °C for **a)** the polymer blend membranes, **b)** the thermally treated Matrimid membranes and **c)** the chemically crosslinked Matrimid membranes. Solid lines between data points are added to guide the eye. Open symbols represent gaseous CO_2 densities, whereas the closed symbols represent liquid-like CO_2 densities. Error bars are small and therefore fall behind the symbols of the data points.

and thus higher CO_2 permeabilities. The transition from gaseous CO_2 densities (open symbols) to liquid-like CO_2 densities (closed symbols) at 80 bar is distinctly visible in the permeation behavior. This change in permeation behavior is attributed to the significantly increasing CO_2 density, as a consequence of the transition to a liquid-like CO_2 density. The CO_2 sorption in Matrimid membranes at sc-CO_2 conditions is closely correlated with the CO_2 density [5,28]. The transition to a liquid-like CO_2 density causes a steep increase in CO_2 density (Fig. 1), which subsequently levels off after the transition occurs. For this reason, the CO_2 sorption reaches a plateau value at liquid-like CO_2 densities and thus the extent of plasticization is independent of the feed pressure in this region. The effect of the transition on the CO_2 sorption and permeation behavior of Matrimid is discussed in more detail in our previous work [5,28]. Although the extent of plasticization is independent of the feed pressure at liquid-like CO_2 densities, the CO_2 permeability still increases linearly as a function of pressure. This is attributed to the large time-dependency of plasticization [3,24,28,55,56]. As the experimental time for each pressure step is relatively short, the membrane keeps plasticizing over time resulting in a continuous increase in permeability over time, independent of the feed pressure [5]. In other words, in the liquid-like CO_2 density region the CO_2 permeability has no pressure dependency, but solely increases over time, which is represented by the linear increase in CO_2 permeability in this liquid-like CO_2 density region for Matrimid.

3.3.1. Polymer blending

Matrimid has a higher CO_2 permeability compared to P84, which is in good agreement with values obtained in literature at low pressures (Fig. 5a) [5,12,57]. The plasticization pressure of Matrimid is around 10 bar, while P84 has its plasticization pressure around 22 bar [1,12,34]. Therefore, the relative permeability, solubility and diffusivity of the blends at 40 bar CO_2 pressure, as shown in Fig. 6, are measured above the plasticization pressure of both pure polymers. The CO_2 permeabilities of the blends are found in between the values of the two pure polymers, where an increasing P84 content results in a decreasing CO_2 permeability [12]. Increasing the P84 content in the blend mostly reduces the diffusivity of CO_2, which is in good agreement with the smaller d-spacing and higher T_g found for the pure P84 polymer. It is clear from Fig. 5a that P84 has a significantly higher resistance to plasticization compared to pristine Matrimid as in the gaseous CO_2 region the increase in CO_2 permeability with feed pressure is extensively reduced. When entering the liquid-like CO_2 density region at 80 bar the CO_2 permeability increases slightly due to the increasing CO_2 density but shows no significant increase in the liquid-like CO_2 density region. This shows that P84 has a high plasticization resistance even at supercritical conditions. All polymer blends show an S-shape permeability curve with its inflection point at the pressure where the transition to a liquid-like CO_2 density occurs (80 bar). It is highly likely that the behavior of Matrimid, the CO_2 sorption reaching a plateau value after the transition occurs, extends to P84 and the blend membranes as similar behavior is observed [5,28]. When the fraction of Matrimid increases in the polymer blend, the permeation behavior resembles more the permeation behavior of pristine Matrimid. The reason for this is that with increasing Matrimid content, the k_D parameter increases resulting in greater CO_2 concentrations at higher pressures. Consequently, the extent of plasticization increases leading to higher CO_2 permeabilities. Especially at 50 and 75 wt% Matrimid, the increase in CO_2 permeability in the gaseous CO_2 region is considerably higher compared to P84. Even more so, in the liquid-like CO_2 density region these blends still show strong plasticization indicated by the higher slope of the permeability curves in the liquid-like CO_2 density region. This indicates that even though the extent of plasticization is reduced compared to pristine Matrimid, the blends with 50 and 75 wt% Matrimid are still highly plasticized in the liquid-like CO_2 density region. The blend with a high ratio of P84, 25-75 M-P84, shows a better resistance to plasticization, but this also results in a large loss in CO_2 permeability.

3.3.2. Thermally treated

Both thermal treatments show a reduced CO_2 permeability at 40 bar of CO_2 feed pressure, although the reduction in permeability is significantly larger for the membranes thermally treated in air (Fig. 7). For the N_2 thermally treated membranes the changes in membrane properties originate from the formation of the CTC's and minor crosslinking, resulting in a decrease in both solubility and diffusivity. In contrast, the membranes treated in air have a higher crosslink density that results in considerably reduced chain mobility and thereby lower diffusivity. Consequently, the larger reduction in CO_2 permeability for the thermally treated membranes in air is mostly attributed to a decreased diffusivity. Even though the d-spacing of the thermally treated membranes is similar (6.05 Å and 6.01 Å for the treatment in N_2 and air respectively), the diffusivity is evidently different due to the thermo-oxidative crosslinking.

The CO_2 permeability as a function of pressure for the thermally treated membranes is shown in Fig. 5b. In the gaseous CO_2 region, the CO_2 permeability of the thermally treated membranes in N_2 increases

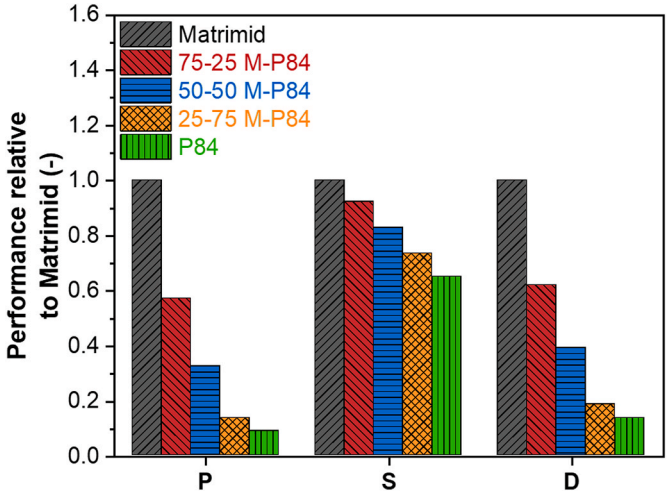

Fig. 6. CO_2 permeability (P), solubility (S) and diffusivity (D) of the pure polymer and polymer blend membranes relative to pristine Matrimid at 35 °C and 40 bar CO_2 feed pressure. The diffusivity values are calculated using the equation of the solution-diffusion model (P═S·D).

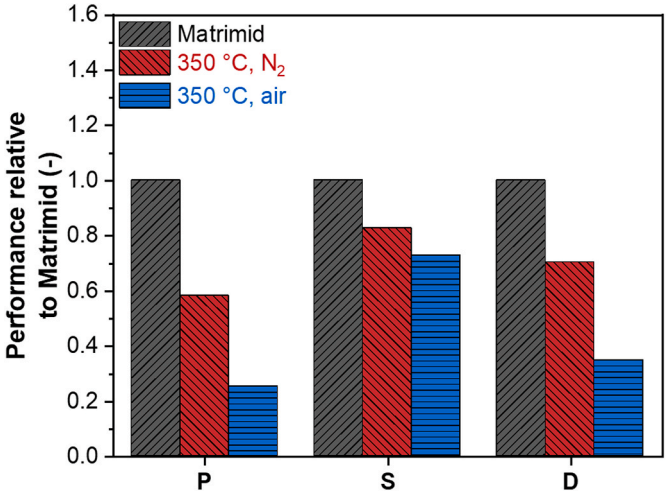

Fig. 7. CO_2 permeability (P), solubility (S) and diffusivity (D) of the thermally treated Matrimid membranes relative to pristine Matrimid at 35 °C and 40 bar CO_2 feed pressure. The diffusivity values are calculated using the equation of the solution-diffusion model (P═S·D).

slightly, while the permeability of the membranes treated in air remains relatively constant. This indicates that the membranes treated in N_2 slightly plasticize, while plasticization is significantly suppressed for the membranes treated in air. This is in agreement with the significantly lower k_D parameters for the thermally treated membranes and results found in literature [6,24]. The difference in performance between the thermally treated membranes is attributed to the higher crosslink density obtained during the thermal treatment in air and the accompanying lower CO_2 sorption. For both membranes the CO_2 permeability exhibits a slight jump around the pressure where the transition to liquid-like CO_2 densities occurs. Near the transition pressure (80 bar), small changes in CO_2 pressure result in significant changes in CO_2 density (Fig. 1), which results in a jump in CO_2 concentration when entering the liquid-like CO_2 density region, as observed for Matrimid in our earlier work [28]. It is unclear if this slight jump in CO_2 permeability is caused by a larger extent of plasticization or by the increased CO_2 solubility as a result in the increasing CO_2 density. However, in the liquid-like CO_2 density region the CO_2 permeability shows only a minor increase for the N_2 thermally treated membrane, while it remains constant for the membrane treated in air. This elucidates that the extent of plasticization is significantly reduced compared to pristine Matrimid and does not increase further with increasing pressure. While thermo-oxidative crosslinking shows a high resistance to plasticization, it comes at the cost of permeability. The formation of CTC's and minor crosslinking during the treatment in N_2 results in a somewhat lower plasticization resistance compared to the treatment in air, but at the same time retains a relatively high permeability.

3.3.3. *Chemically crosslinked*

Fig. 8 shows the relative CO_2 permeability, solubility and diffusivity of the chemically crosslinked Matrimid membranes to pristine Matrimid. The reduced permeability of the m-PDA crosslinked membranes is mostly determined by the lower diffusivity due to the crosslinked surface. The slight decrease in permeability for the 7-day m-PDA crosslinked membranes is completely caused by a lower CO_2 sorption, as the diffusivity remains constant. This is in line with the found membrane properties as the longer crosslinking time mostly resulted in a higher amount of m-PDA grafted on the polyimide chains rather than a higher crosslinking density. On the other hand, crosslinking the Matrimid membrane with HMDA for 1 day resulted in a higher initial solubility due to the redistribution of the Langmuir and Henry sorption sites. This shows that the reduced CO_2 permeability is completely caused by a decreased diffusivity due to the lower chain mobility of the crosslinked membranes. In contrast to crosslinking with m-PDA, the CO_2 permeability drops significantly when increasing the crosslinking time from 1 day to 7 days for HMDA crosslinked membranes. The higher crosslink density causes a considerable reduction in chain mobility, indicated with a greater T_g (Table 6). Together with the small d-spacing this results in a high diffusion resistance, and thus a low CO_2 permeability.

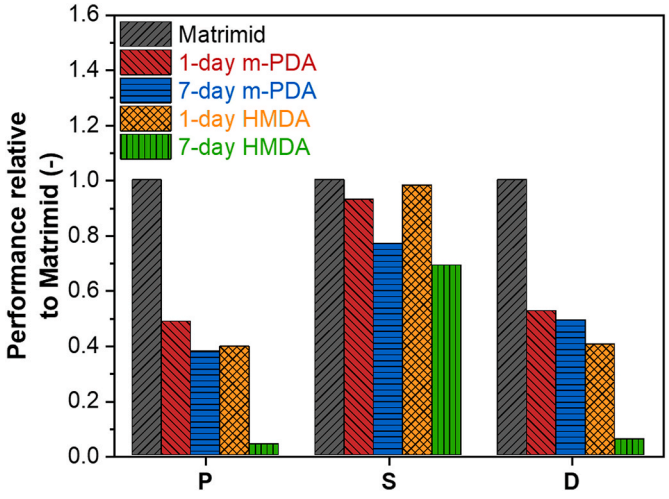

Fig. 8. CO_2 permeability (P), solubility (S) and diffusivity (D) of the chemically crosslinked Matrimid membranes relative to pristine Matrimid at 35 °C and 40 bar CO_2 feed pressure. The diffusivity values are calculated using the equation of the solution-diffusion model (P═S·D).

The CO_2 permeability as a function of pressure for the chemically crosslinked membranes is presented in Fig. 5c. The m-PDA crosslinked membranes show both an increased plasticization resistance compared to pristine Matrimid. However, both membranes still show a relatively large increase in CO_2 permeability in both the gaseous and liquid-like CO_2 density region. In addition, the m-PDA crosslinked membranes show a similar trend in permeation, regardless of crosslinking time, even though the CO_2 sorption for the 7-day crosslinked membrane is lower compared to the 1-day crosslinked membrane. It is possible that the lower CO_2 sorption is countered with a higher chain mobility (indicated with the slightly lower T_g) due to the higher amount of grafted m-PDA after 7 days of crosslinking, resulting in a similar plasticization resistance. Surprisingly, the 1-day HMDA crosslinked membrane shows a similar permeation trend to the m-PDA membranes as a function of pressure, even though the crosslink density throughout the membrane is higher. This is explained by the similar k_D parameter found for the 1-day HMDA crosslinked membrane compared to the m-PDA crosslinked membranes. This confirms that the extent of plasticization is closely correlated to the dissolution of CO_2 between the polymers, even in the liquid-like CO_2 density region. Moreover, even though the diffusivity is lower due to crosslinking, the higher solubility due to the redistribution of the Langmuir and Henry sorption sites retains a relatively high permeability for the 1-day HMDA crosslinked membrane. This results in comparable permeation behavior for the 1-day HMDA crosslinked membrane and the m-PDA crosslinked membranes. The higher crosslink density obtained at 7 days HMDA crosslinking resulted in a significant lower d-spacing and increased T_g, which caused a low initial CO_2 permeability. In addition, a low k_D parameter caused a considerable reduction in the extent of plasticization as the increase in CO_2 permeability as a function of pressure is very small in both the gaseous and liquid-like CO_2 density region. In literature similar behavior is observed at relatively low pressures, where a higher crosslinking degree resulted in a stronger plasticization resistance at the cost of permeability [14,23,45]. All the crosslinked membranes show an S-shape permeability curve with the inflection point around the transition pressure, similar as observed for the polymer blends and the thermally treated membranes, where the S-shape flattens with higher plasticization resistance.

3.4. *Evaluation of the different methods to suppress plasticization at supercritical conditions*

When the different methods to suppress plasticization are compared, it is clear that all membranes show a similar S-shape permeability curve as a function of pressure. However, the plasticization resistance of the membrane determines the extent of the exponential permeability increase in the gaseous CO_2 region and the linear permeability increase in the liquid-like CO_2 density region. The presence of this S-shape behavior for all membranes elucidates that the fluid properties of the sc-CO_2, most importantly the CO_2 density, have a significant influence on plasticization and the corresponding permeation behavior of these membranes. In our earlier work, it was shown that the CO_2 concentration in Matrimid reaches a plateau value in the liquid-like CO_2 density region, because the CO_2 density levels off [28]. It is hypothesized that this is also the case for the treated membranes in this work, as the treated membranes show similar behavior compared to pristine Matrimid, but that the plateau value is different for all treated membranes. This plateau value of the CO_2 concentration is an important parameter determining the swelling stresses, and thus the extent of plasticization, in the liquid-like CO_2 density region. However, the extent of plasticization is not simply

determined by the absolute value of the CO_2 concentration, as sorption in the excess free volume (Langmuir sorption sites) does not contribute to plasticization [21,52,53]. This is further substantiated by the analysis of the CO_2 sorption and the dual-mode sorption parameters of the treated membranes. As an example, the CO_2 concentrations of pristine Matrimid and the 1-day HMDA crosslinked Matrimid are very similar, but the extent of plasticization as a function of pressure for these two membranes is completely different. The reason for this is that the distribution of the Langmuir and Henry sorption sites in these membranes is different, where Matrimid has a higher sorption in the Henry sorption sites (k_D parameter) and the 1-day HMDA crosslinked membranes have a higher sorption in the Langmuir sorption sites (C'_H parameter). This shows that the CO_2 concentration alone is not sufficient and that the dual-mode sorption parameters are required to analyze plasticization. Accordingly, the treated membranes with a low k_D parameter combined with a reduced chain mobility exhibit not only a high resistance to plasticization in the gaseous region, but also in the liquid-like region.

Pristine P84 membranes show a high plasticization resistance even in the liquid-like CO_2 density region, therefore blending Matrimid with P84 is an effective way to increase the plasticization resistance at low pressures, as also observed in literature [12,58]. There is a clear correlation between the d-spacing and the k_D parameter for the blends. The blends with a higher P84 content have a lower d-spacing and thus a reduced k_D parameter. This reduced k_D parameter results in a higher resistance to plasticization. However, high amounts of P84 are required to suppress plasticization at liquid-like CO_2 density conditions, consequently the permeability also drops significantly. Increasing the amount of P84 in the polymer blend only results in extra intrachain rigidity, but also interchain rigidity is required to withstand the large plasticization stresses at high CO_2 pressures and supercritical conditions [4,5,21]. Crosslinking provides this additional interchain rigidity. The thermally treated membranes in air and the 7-day HMDA crosslinked membranes exhibit a high degree of crosslinking and thus interchain rigidity, indicated with a high T_g, high gel content and a low k_D parameter. Accordingly, these membranes show the highest resistance to plasticization. Even though the plasticization resistance is similar for these two membranes, the absolute permeability is significantly lower for the HMDA crosslinked membrane compared to the thermo-oxidatively crosslinked membrane. This is attributed to the larger degree of crosslinking of the 7-day HMDA crosslinked membrane, which resulted in a significantly lower d-spacing and k_D parameter. Therefore, the degree of crosslinking not only determines the plasticization resistance, but also the absolute permeabilities. Surprisingly, the N_2 thermally treated membranes, which are not highly crosslinked (gel content 60%), exhibit significant plasticization resistance even in the liquid-like CO_2 density region, while retaining a high permeability. Even more, compared to the 1-day HMDA crosslinked membranes, which are more crosslinked (gel content of 85%), the N_2 thermally treated membranes show a higher plasticization resistance combined with a higher permeability. The formation of CTC's during the thermal treatment in N_2 results in an increase in interchain rigidity, indicated with a significant increase in T_g for these membranes, while the d-spacing only decreases marginally compared to Matrimid. This illustrates that the formation of the CTC's during the thermal treatment has a significant contribution towards the plasticization resistance of these thermally treated membranes. Crosslinking of the membrane surface with the bulky m-PDA crosslinker increases the plasticization resistance compared to pristine Matrimid but is not sufficient to effectively suppress plasticization especially in the liquid-like CO_2 density region. These results show that all three different methods, blending, thermal treatments and chemically crosslinking are capable of suppressing plasticization at high CO_2 pressures and supercritical conditions. Although, chemical crosslinking and the thermal treatments are found to be more superior in plasticization suppression, especially in the liquid-like CO_2 density region.

4. Conclusions

Polymer blending, thermal treatments and chemical crosslinking approaches were used to suppress plasticization in Matrimid based polyimide membranes at high CO_2 pressures and supercritical conditions. The resulting membranes were characterized to identify possible chemical modifications as well as to determine the density, glass transition temperature, gel content and d-spacing of the membranes. Next, all membranes were evaluated for their membrane performance properties: CO_2 sorption, CO_2 permeation and corresponding plasticization behavior. It was found that all methods applied reduced the intra- and interchain mobility by decreasing the d-spacing and/or increasing the T_g of the membranes. Crosslinking proved to be the most effective method to decrease intra- and interchain mobility. CO_2 sorption measurements showed that especially sorption in the Henry sorption sites promoted plasticization, which demonstrated that the absolute CO_2 concentration alone is not enough to analyze plasticization phenomena. Lower d-spacings and higher T_g's resulted in a lower k_D parameter and thus a better resistance to plasticization. This showed that the d-spacing and chain mobility are key parameters to suppress plasticization. Furthermore, the fluid properties of sc-CO_2, specifically the CO_2 density, have a significant influence on the plasticization behavior. In the liquid-like CO_2 density region the swelling stresses were considerably stronger compared to swelling stresses in the gaseous region. Consequently, a strong interchain rigidity was required to suppress plasticization under these liquid-like CO_2 densities. Chemically crosslinking with HMDA and thermo-oxidative crosslinking showed the most significant decrease in interchain mobility and thus increase in plasticization resistance, but the increase in plasticization resistance comes at the expense of the permeability. Even though the thermal treatment in N_2 led to a lower crosslinking density, the membranes only displayed a slightly lower plasticization resistance due to the formation of CTC's, while retaining a high permeability. This illustrates the potential of CTC's in these polyimide membranes for the combination of plasticization suppression and high permeabilities. High ratios of P84 in the Matrimid blends were required to effectively suppress the plasticization at high CO_2 pressures, which also led to a greatly decreased permeability. These results strongly highlight that all three different methods, blending, thermal treatments and chemical crosslinking are able to suppress plasticization at high CO_2 pressures, but that proper tailoring strategies are able to increase the plasticization resistance while maintaining high permeabilities.

CRediT authorship contribution statement

Menno Houben: Conceptualization, Methodology, Validation, Formal analysis, Investigation, Writing – Original Draft, Writing – Review & Editing, Visualization. **Joey Kloos:** Formal analysis, Investigation, Writing - review & editing. **Machiel van Essen:** Formal analysis, Writing - review & editing. **Kitty Nijmeijer:** Conceptualization, Supervision, Writing - review & editing, Project administration, Funding acquisition. **Zandrie Borneman:** Conceptualization, Supervision, Writing - review & editing, Project administration, Funding acquisition.

Declaration of competing interest

The authors declare that they have no known competing financial interests or personal relationships that could have appeared to influence the work reported in this paper.

Acknowledgements

This research did not receive any specific grant from funding agencies in the public, commercial, or not-for-profit sectors. The authors wish to express their gratitude to Wetsus, Centre of Excellence for Sustainable Water Technology, for providing the high-pressure permeation

equipment and Anna Casimiro from the Eindhoven University of Technology for her help with the WAXS measurements.

Appendix A. Supplementary data

Supplementary data to this article can be found online at https://doi.org/10.1016/j.memsci.2022.120292.

References

[1] A. Bos, I.G.M. Pünt, M. Wessling, H. Strathmann, CO_2-induced plasticization phenomena in glassy polymers, J. Membr. Sci. 155 (1999) 67–78, https://doi.org/10.1016/S0376-7388(98)00299-3.

[2] M. Wessling, S. Schoeman, T. van der Boomgaard, C.A. Smolders, Plasticization of gas separation membranes, Gas Separ. Purif. 5 (1991) 222–228, https://doi.org/10.1016/0950-4214(91)80028-4.

[3] M. Wessling, I. Huisman, T. van der Boomgaard, C.A. Smolders, Time-dependent permeation of carbon dioxide through a polyimide membrane above the plasticization pressure, J. Appl. Polym. Sci. 58 (1995) 1959–1966, https://doi.org/10.1002/app.1995.070581105.

[4] J.D. Wind, S.M. Sirard, D.R. Paul, P.F. Green, K.P. Johnston, W.J. Koros, Carbon dioxide-induced plasticization of polyimide membranes: pseudo-equilibrium relationships of diffusion, sorption, and swelling, Macromolecules 36 (2003) 6433–6441, https://doi.org/10.1021/ma0343582.

[5] M. Houben, R. van Geijn, M. van Essen, Z. Borneman, K. Nijmeijer, Supercritical CO_2 permeation in glassy polyimide membranes, J. Membr. Sci. 620 (2021) 118922, https://doi.org/10.1016/j.memsci.2020.118922.

[6] A. Bos, I.G.M. Pünt, M. Wessling, H. Strathmann, Plasticization-resistant glassy polyimide membranes for CO_2/CH_4 separations, Separ. Purif. Technol. 14 (1998) 27–39, https://doi.org/10.1016/S1383-5866(98)00057-4.

[7] S. Shahid, K. Nijmeijer, Performance and plasticization behavior of polymer-MOF membranes for gas separation at elevated pressures, J. Membr. Sci. 470 (2014) 166–177, https://doi.org/10.1016/j.memsci.2014.07.034.

[8] J.K. Adewole, A.L. Ahmad, Polymeric membrane materials selection for high-pressure CO_2 removal from natural gas, J. Polym. Res. 24 (2017) 70, https://doi.org/10.1007/s10965-017-1231-6.

[9] A.L. Lee, H.L. Feldkirchner, S.A. Stern, A.Y. Houde, J.P. Gamez, H.S. Meyer, Field tests of membrane modules for the separation of carbon dioxide from low-quality natural gas, Gas Separ. Purif. 9 (1995) 35–43, https://doi.org/10.1016/0950-4214(95)92175-C.

[10] M. Mazzotti, R. Pini, G. Storti, Enhanced coalbed methane recovery, J. Supercrit. Fluids 47 (2009) 619–627, https://doi.org/10.1016/j.supflu.2008.08.013.

[11] Y. Chu, X. He, Process simulation and cost evaluation of carbon membranes for CO_2 removal from high-pressure natural gas, Membranes 8 (2018), https://doi.org/10.3390/membranes8040118.

[12] A. Bos, I. Pünt, H. Strathmann, M. Wessling, Suppression of gas separation membrane plasticization by homogeneous polymer blending, AIChE J. 47 (2001) 1088–1093, https://doi.org/10.1002/aic.690470515.

[13] G.C. Kapantaidakis, G.H. Koops, M. Wessling, CO_2 plasticization of polyethersulfone/polyimide gas-separation membranes, AIChE J. 49 (2003), https://doi.org/10.1002/aic.690490710.

[14] P.S. Tin, T.S. Chung, Y. Liu, R. Wang, S.L. Liu, K.P. Pramoda, Effects of cross-linking modification on gas separation performance of Matrimid membranes, J. Membr. Sci. 225 (2003) 77–90, https://doi.org/10.1016/j.memsci.2003.08.005.

[15] C. Staudt-Bickel, W.J. Koros, Improvement of CO_2/CH_4 separation characteristics of polyimides by chemical crosslinking, J. Membr. Sci. 155 (1999) 145–154, https://doi.org/10.1016/S0376-7388(98)00306-8.

[16] M.E. Dose, M. Chwatko, I. Hubacek, N.A. Lynd, D.R. Paul, B.D. Freeman, Thermally cross-linked diaminophenylindane (DAPI) containing polyimides for membrane based gas separations, Polymer (Guildf) 161 (2019) 16–26, https://doi.org/10.1016/j.polymer.2018.11.050.

[17] X. Duthie, S. Kentish, S.J. Pas, A.J. Hill, C. Powell, K. Nagai, G. Stevens, G. Qiao, Thermal treatment of dense polyimide membranes, J. Polym. Sci., Part B: Polym. Phys. 46 (2008) 1879–1890, https://doi.org/10.1002/polb.21521.

[18] H. Kita, T. Inada, K. Tanaka, K. Okamoto, Effect of photocrosslinking on permeability and permselectivity of gases through benzophenone- containing polyimide, J. Membr. Sci. 87 (1994) 139–147, https://doi.org/10.1016/0376-7388(93)E0098-X.

[19] S. Matsui, T. Nakagawa, Effect of ultraviolet light irradiation on gas permeability in polyimide membranes. II. Irradiation of membranes with high-pressure mercury lamp, J. Appl. Polym. Sci. 67 (1998) 49–60, https://doi.org/10.1002/(SICI)1097-4628(19980103)67:1<49::AID-APP6>3.0.CO;2-O.

[20] M. Zhang, L. Deng, D. Xiang, B. Cao, S.S. Hosseini, P. Li, Approaches to suppress CO_2-induced plasticization of polyimide membranes in gas separation applications, Processes 7 (2019), https://doi.org/10.3390/pr7010051.

[21] J.D. Wind, C. Staudt-Bickel, D.R. Paul, W.J. Koros, The effects of crosslinking chemistry on CO_2 plasticization of polyimide gas separation membranes, Ind. Eng. Chem. Res. 41 (2002) 6139–6148, https://doi.org/10.1021/ie0204639.

[22] L. Shao, L. Liu, S.X. Cheng, Y.D. Huang, J. Ma, Comparison of diamino cross-linking in different polyimide solutions and membranes by precipitation observation and gas transport, J. Membr. Sci. 312 (2008) 174–185, https://doi.org/10.1016/j.memsci.2007.12.060.

[23] S.J. Kim, Y. Ahn, J.F. Kim, S.E. Nam, H. Park, Y.H. Cho, K. youl Baek, Y.I. Park, Comparison of liquid-phase and methanol-swelling crosslinking processes of polyimide dense membrane for CO_2/CH_4 separation, J. Appl. Polym. Sci. 138 (2021), https://doi.org/10.1002/app.49860.

[24] G. Dong, H. Li, V. Chen, Plasticization mechanisms and effects of thermal annealing of Matrimid hollow fiber membranes for CO_2 removal, J. Membr. Sci. 369 (2011) 206–220, https://doi.org/10.1016/j.memsci.2010.11.064.

[25] F. Zhou, W.J. Koros, Study of thermal annealing on Matrimid® fiber performance in pervaporation of acetic acid and water mixtures, Polymer (Guildf) 47 (2006) 280–288, https://doi.org/10.1016/j.polymer.2005.11.017.

[26] M. Hasegawa, I. Mita, M. Kochi, R. Yokota, Charge-transfer emission spectra of aromatic polyimides, J. Polym. Sci. C Polym. Lett. 27 (1989) 263–269, https://doi.org/10.1002/pol.1989.140270804.

[27] S.R. Reijerkerk, K. Nijmeijer, C.P. Ribeiro, B.D. Freeman, M. Wessling, On the effects of plasticization in CO_2/light gas separation using polymeric solubility selective membranes, J. Membr. Sci. 367 (2011) 33–44, https://doi.org/10.1016/j.memsci.2010.10.035.

[28] M. Houben, M. van Essen, K. Nijmeijer, Z. Borneman, Time-dependent plasticization behavior of polyimide membranes at supercritical conditions, J. Membr. Sci. 635 (2021) 119512, https://doi.org/10.1016/j.memsci.2021.119512.

[29] Thermophysical Properties of Fluid Systems - NIST, National Institute of Standards and Technology, 2016. http://webbook.nist.gov/chemistry/fluid/. (Accessed 5 April 2017).

[30] A. Shamu, M. Dunnewold, H. Miedema, Z. Borneman, K. Nijmeijer, Permeation of supercritical CO_2 through dense polymeric membranes, J. Supercrit. Fluids 144 (2019) 63–70, https://doi.org/10.1016/j.supflu.2018.10.009.

[31] G.G. Simeoni, T. Bryk, F.A. Gorelli, M. Krisch, G. Ruocco, M. Santoro, T. Scopigno, The Widom line as the crossover between liquid-like and gas-like behaviour in supercritical fluids, Nat. Phys. 6 (2010) 503–507, https://doi.org/10.1038/nphys1683.

[32] A.R. Imre, C. Ramboz, U.K. Deiters, T. Kraska, Anomalous fluid properties of carbon dioxide in the supercritical region: application to geological CO_2 storage and related hazards, Environ. Earth Sci. 73 (2015) 4373–4384, https://doi.org/10.1007/s12665-014-3716-5.

[33] C. Cockrell, V.V. Brazhkin, K. Trachenko, Transition in the supercritical state of matter : review of experimental evidence, Phys. Rep. 941 (2021) 1–27, https://doi.org/10.1016/j.physrep.2021.10.002.

[34] M. Houben, Z. Borneman, K. Nijmeijer, Plasticization behavior of crown-ether containing polyimide membranes for the separation of CO_2, Separ. Purif. Technol. 255 (2021) 117307, https://doi.org/10.1016/j.seppur.2020.117307.

[35] G. Soave, M. Barolo, A. Bertucco, Estimation of high-pressure fugacity coefficients of pure gaseous fluids by a modified SRK equation of state, Fluid Phase Equil. 91 (1993) 87–100, https://doi.org/10.1016/0378-3812(93)85081-V.

[36] G.G. Kapantaidakis, S.P. Kaldis, X.S. Dabou, G.P. Sakellaropoulos, Gas permeation through PSF-PI miscible blend membranes, J. Membr. Sci. 110 (1996) 239–247, https://doi.org/10.1016/0376-7388(95)00265-0.

[37] A.Y. Houde, S.S. Kulkarni, M.G. Kulkarni, Permeation and plasticization behavior of glassy polymers: a WAXD interpretation, J. Membr. Sci. 71 (1992) 117–128, https://doi.org/10.1016/0376-7388(92)85011-7.

[38] S.G. Charati, A.Y. Houde, S.S. Kulkarni, M.G. Kulkarni, Transport of gases in aromatic polyesters: correlation with WAXD studies, J. Polym. Sci., Part B: Polym. Phys. 29 (1991) 921–931, https://doi.org/10.1002/polb.1991.090290803.

[39] R. Thür, V. Lemmens, D. Van Havere, M. van Essen, K. Nijmeijer, I.F. J. Vankelecom, Tuning 6FDA-DABA membrane performance for CO_2 removal by physical densification and decarboxylation cross-linking during simple thermal treatment, J. Membr. Sci. 610 (2020) 118195, https://doi.org/10.1016/j.memsci.2020.118195.

[40] W. Qiu, C. Chen, L. Xu, L. Cui, D.R. Paul, W.J. Koros, Sub-tg cross-linking of a polyimide membrane for enhanced CO_2 plasticization resistance for natural gas separation, Macromolecules 44 (2011) 6046–6056, https://doi.org/10.1021/ma201033j.

[41] J.N. Barsema, S.D. Klijnstra, J.H. Balster, N.F.A. Van Der Vegt, G.H. Koops, M. Wessling, Intermediate polymer to carbon gas separation membranes based on Matrimid PI, J. Membr. Sci. 238 (2004) 93–102, https://doi.org/10.1016/j.memsci.2004.03.024.

[42] S. Kuroda, I. Mita, Degradation of aromatic polymers-II. The crosslinking during thermal and thermo-oxidative degradation of a polyimide, Eur. Polym. J. 25 (1989) 611–620, https://doi.org/10.1016/0014-3057(89)90014-1.

[43] S. Yi, B. Ghanem, Y. Liu, I. Pinnau, W.J. Koros, Ultraselective glassy polymer membranes with unprecedented performance for energy-efficient sour gas separation, Sci. Adv. 5 (2019) 1–12, https://doi.org/10.1126/sciadv.aaw5459.

[44] N.R. Horn, D.R. Paul, Carbon dioxide plasticization of thin glassy polymer films, Polymer 52 (2011) 5587–5594, https://doi.org/10.1016/j.polymer.2011.10.004.

[45] M.R. Rahmani, A. Kazemi, F. Talebnia, G. Khanbabaei, Preparation and characterization of cross-linked Matrimid membranes for CO_2/CH_4 separation, Polym. Sci. B 56 (2014) 650–656, https://doi.org/10.1134/S1560090414050108.

[46] X. Qiao, T. Chung, Diamine modification of P84 polyimide membranes for pervaporation dehydration of isopropanol, AIChE J. 52 (2006) 3462–3472, https://doi.org/10.1002/aic.

[47] B. Dao, A.M. Groth, J. Hodgkin, Differential reactivity of aromatic diamines during polyimide formation in water, Eur. Polym. J. 45 (2009) 1607–1616, https://doi.org/10.1016/j.eurpolymj.2008.12.012.

[48] A.J. Erb, D.R. Paul, Gas sorption and transport in polysulfone, J. Membr. Sci. 8 (1981) 11–22, https://doi.org/10.1016/S0376-7388(00)82135-3.

[49] S. Kanehashi, K. Nagai, Analysis of dual-mode model parameters for gas sorption in glassy polymers, J. Membr. Sci. 253 (2005) 117–138, https://doi.org/10.1016/j.memsci.2005.01.003.
[50] W.R. Vieth, J.M. Howell, J.H. Hsieh, Dual sorption theory, J. Membr. Sci. 1 (1976) 177–220, https://doi.org/10.1016/S0376-7388(00)82267-X.
[51] E. Ricci, M.G. De Angelis, Modelling mixed-gas sorption in glassy polymers for CO_2 removal: a sensitivity analysis of the dual mode sorption model, Membranes 9 (2019) 1–26, https://doi.org/10.3390/membranes9010008.
[52] M.R. Coleman, W.J. Koros, Conditioning of fluorine containing polyimides. 1. Effect of exposure to high pressure carbon dioxide on permeability, Macromolecules 30 (1997) 6899–6905, https://doi.org/10.1021/ma961323b.
[53] M.R. Coleman, W.J. Koros, Conditioning of fluorine-containing polyimides. 2. Effect of conditioning protocol at 8% volume dilation on gas-transport properties, Macromolecules 32 (1999) 3106–3113, https://doi.org/10.1021/ma981376o.
[54] E.J. Kappert, M.J.T. Raaijmakers, K. Tempelman, F.P. Cuperus, W. Ogieglo, N. E. Benes, Swelling of 9 polymers commonly employed for solvent-resistant nanofiltration membranes: a comprehensive dataset, J. Membr. Sci. 569 (2019) 177–199, https://doi.org/10.1016/j.memsci.2018.09.059.
[55] S. Kanehashi, T. Nakagawa, K. Nagai, X. Duthie, S. Kentish, G. Stevens, Effects of carbon dioxide-induced plasticization on the gas transport properties of glassy polyimide membranes, J. Membr. Sci. 298 (2007) 147–155, https://doi.org/10.1016/j.memsci.2007.04.012.
[56] J.D. Wind, S.M. Sirard, D.R. Paul, P.F. Green, K.P. Johnston, W.J. Koros, Relaxation dynamics of CO_2 diffusion, sorption, and polymer swelling for plasticized polyimide membranes, Macromolecules 36 (2003) 6442–6448, https://doi.org/10.1021/ma034359u.
[57] P.S. Tin, T.S. Chung, Y. Liu, R. Wang, Separation of CO_2/CH_4 through carbon molecular sieve membranes derived from P84 polyimide, Carbon N. Y. 42 (2004) 3123–3131, https://doi.org/10.1016/j.carbon.2004.07.026.
[58] T. Visser, N. Masetto, M. Wessling, Materials dependence of mixed gas plasticization behavior in asymmetric membranes, J. Membr. Sci. 306 (2007) 16–28, https://doi.org/10.1016/j.memsci.2007.07.048.